

## Ionicity-dependent proton-coupled electron transfer of supramolecular self-assembled electroactive heterocycles

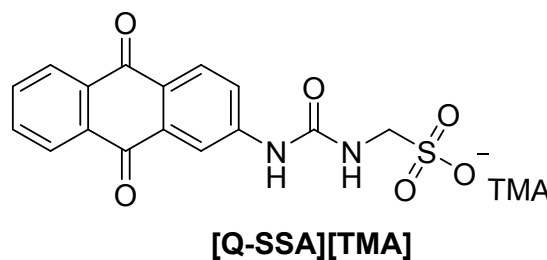
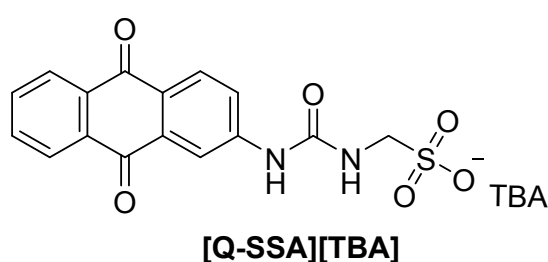
Kendrick K. L. Ng, Reema Devlia, Nichola L. Foss, Luke S. Alesbrook, Jennifer R. Hiscock, and Alexander T. Murray, School of Physical Sciences, University of Kent, Canterbury, UK, CT2 7NH; Email: j.hiscock@kent.ac.uk, a.t.murray@kent.ac.uk,

### Electronic Supplementary information

Contents

<b>Compound structure</b> .....	1
<b>General experimental</b> .....	2
<b>Electrochemistry data</b> .....	5
<b>DLS data</b> .....	8
<b>Zeta potential data</b> .....	12
<b>Synthesis</b> .....	15
<b>Compound characterisation</b> .....	16
<b>References</b> .....	22

### Compound structure



## General experimental

A positive pressure of nitrogen and oven dried glassware were used for all reactions. All solvents and starting materials were purchased from known chemical suppliers or available stores and used without any further purification unless specifically stipulated. NMR spectra were obtained using a Bruker AV2 400 MHz or AVNEO 400 MHz spectrometer. The data was processed using ACD Labs and Topspin software. NMR Chemical shift values are reported in parts per million (ppm) and calibrated to the centre of the residual solvent peak set (s = singlet, br = broad, d = doublet, t = triplet, q = quartet, m = multiplet). The melting point for each compound was measured using Stuart SMP10 melting point apparatus. High-resolution mass spectrometry was performed using a Bruker microTOF-Q mass spectrometer and spectra recorded and processed using Bruker's Compass Data Analysis software. Infrared spectra were obtained using a Shimadzu IR-Affinity-1 model Infrared spectrometer. The data are analysed in wavenumbers ( $\text{cm}^{-1}$ ) using IRsolution software. DLS and Zeta Potential studies were carried out using Anton Paar Litesizer<sup>TM</sup> 500 and processed using Kalliope<sup>TM</sup>. SEM analysis was performed using a Hitachi S3400 N scanning electron microscope, with a 20 Kv accelerating voltage at a vacuum level of <1 pa. The corresponding images were processed using Oxford Instruments AZtex software.

**Voltammetric studies:** Cyclic voltammetry studies were performed using a BioLogic VMP3 multi-channel potentiostat. All measurements were conducted at ambient temperature ( $21 \pm 1$  °C) under nitrogen, in deionised water using a 3 mm glassy carbon electrode (CHI), platinum wire reference electrode (Alfa Aesar, 99.99%), and an Ag/AgCl reference electrode (CHI). Ag/AgCl reference electrodes were stored in 3 M KCl and periodically checked for potential drift against pristine reference electrodes. The working electrode was sequentially polished using 6  $\mu\text{m}$  and 1  $\mu\text{m}$  nano-diamond slurry solution, then 0.05  $\mu\text{m}$  alumina slurry, with sequential rinses in deionised water between polishes. Solutions were made up for cyclic

voltammetry by pH-adjusting an 0.1 M NaOAc solution using a minimum of 1 M NaOH to pH 3.5. 0.3 M quinone was then dissolved in the solution. The solutions were heated to 50 °C for one hour and then cooled to rt to ensure complete solution homogeneity. Filtered solutions were found to have the same electrochemical response as unfiltered solutions. Uncompensated resistance was compensated at 85% using positive feedback. Rotating disk voltammetry was performed using a Metrohm Autolab RDE setup, with a removable 3 mm glassy carbon electrode (Metrohm) which was polished in the usual fashion.

**Mass Spectrometry:** Approximately 1 mg of each compound was dissolved in 1 mL of methanol. This solution was further diluted 100-fold before undergoing analysis where 10  $\mu$ L of each sample was then injected directly into a flow of 10 mM ammonium acetate in 95 % water (flow rate = 0.02 mL/min).

**DLS Studies:** All vials used for preparing the samples were clean dry. All solvents used were filtered to remove any particulates that may interfere with the results obtained. All samples underwent an annealing process, in which they were heated to 40 °C before being allowed to cool to 25 °C. A series of 9 or 10 runs were recorded at 25 °C.

**Zeta Potential Studies:** All vials used for preparing the samples were clean dry. All solvents used were filtered to remove any particulates that may interfere with the results obtained. All samples underwent an annealing process in which the various solutions were heated to approximately 40 °C before cooling to room temperature, allowing each sample to reach a thermodynamic minimum. The final zeta potential value given is an average of the number of experiments conducted at 25 °C.

**Scanning Electron Microscopy (SEM) sample preparation:** A sample containing the compound (1 mg) in the appropriate salt solution (20 mL, 0.1 M NaOAc adjusted to pH 4 with 1 M HCl, or the same with 0.9 M NaCl) was dehydrated slowly at 50 °C over 4 days. The sample was then positioned on a carbon tab, which was then mounted on an aluminium stub.

## Electrochemistry data

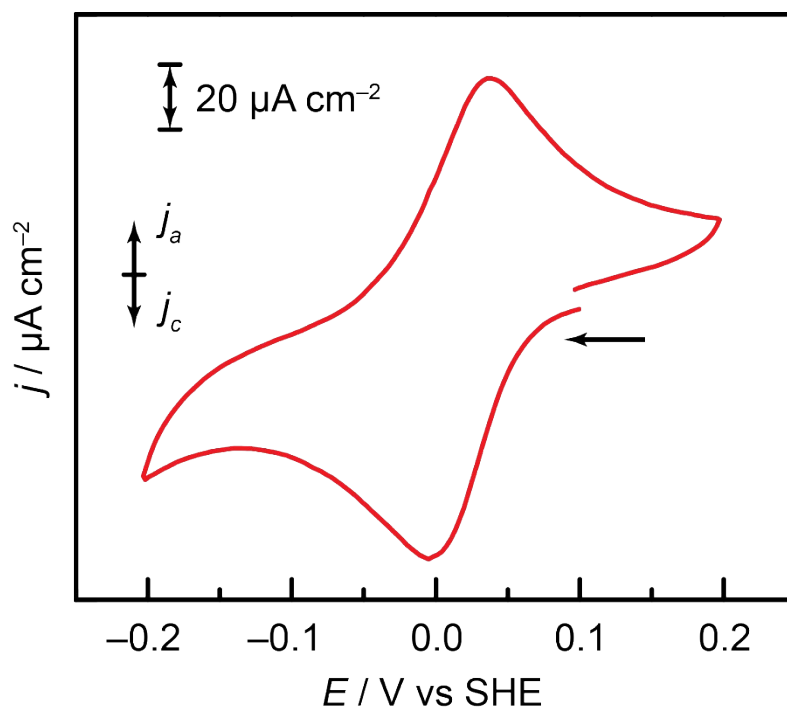


**Figure S1.** Cyclic voltammogram ( $50 \text{ mV s}^{-1}$ ) of [Q-SSA][TBA] in  $1 \text{ M H}_2\text{SO}_4$

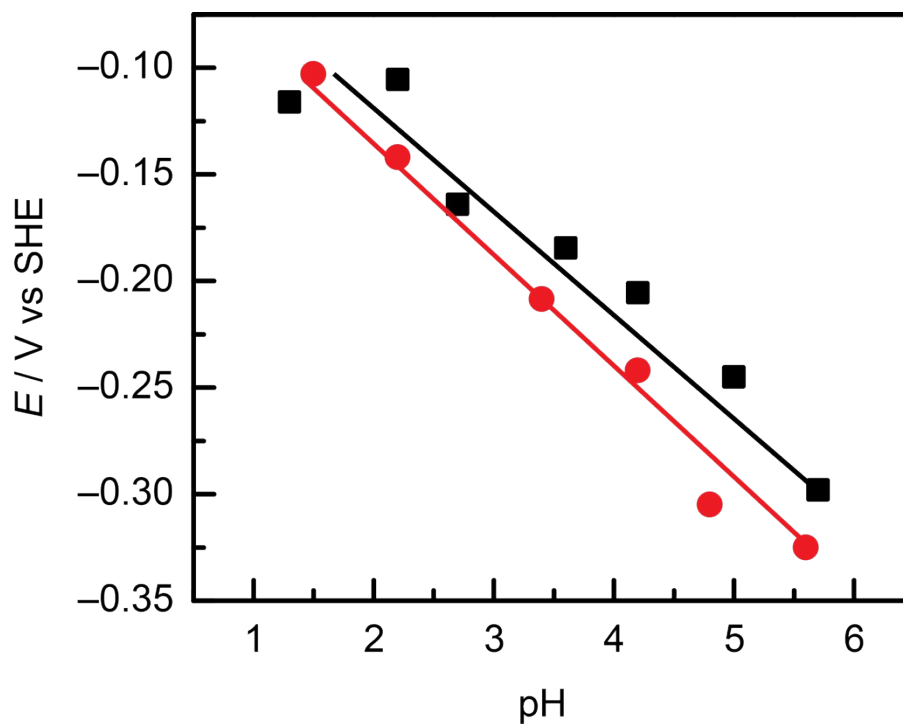


**Figure S2.** Relationship of half-wave potential to pH for [Q-SSA][TBA] in  $0.1 \text{ M NaOAc}$  (black,  $42 \text{ mV/pH}$ ) and  $0.1 \text{ M NaOAc} + 0.9 \text{ M NaCl}$  (red,  $56 \text{ mV/pH}$ )

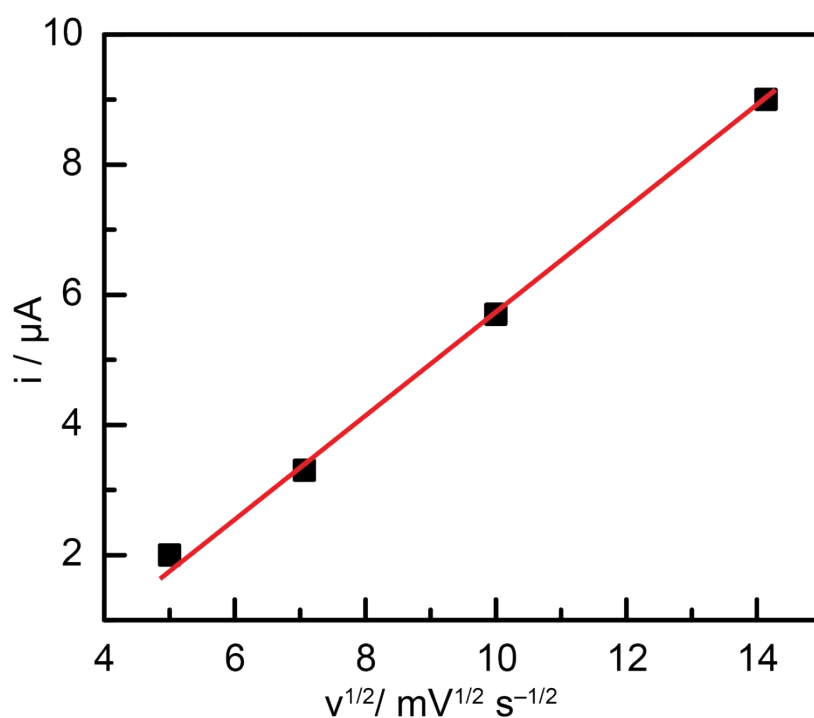


**Figure S3.** Plot of square root of scan rate against peak height for [Q-SSA][TBA], showing linear relationship as expected for freely diffusing molecule.

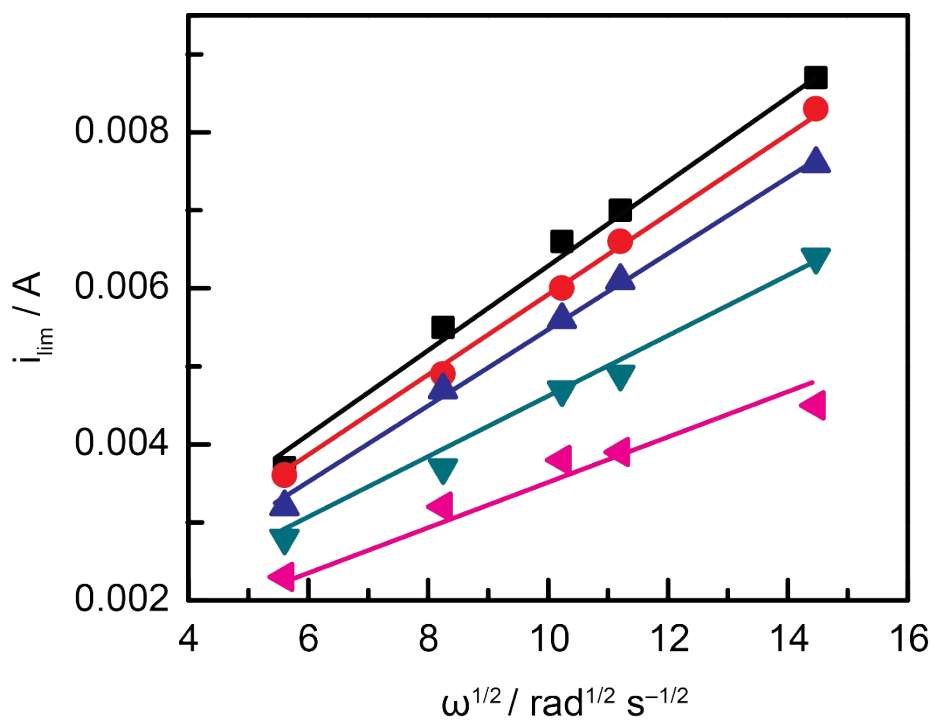


**Figure S4.** Levich plots derived from linear sweep voltammograms taken of [Q-SSA][TBA] with a rotating disk electrode, showing limiting current against the square root of the rotation rate.

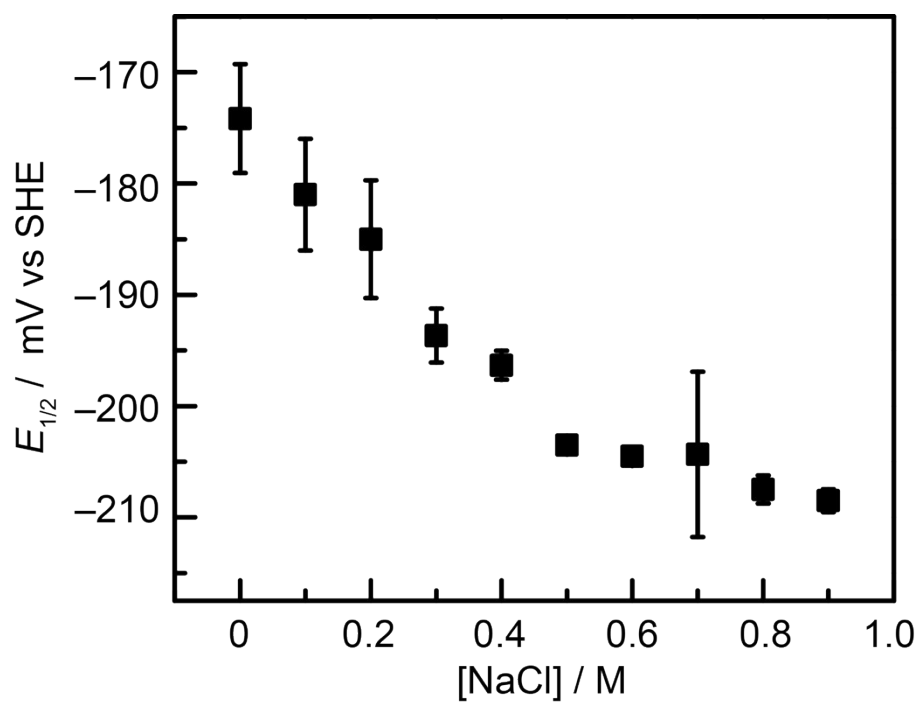


**Figure S5.**  $E_{1/2}$  vs [NaCl] for [Q-SSA][TMA] taken from cyclic voltammograms at 50 mV/sec, at pH 4 in 0.1 M acetate buffer.

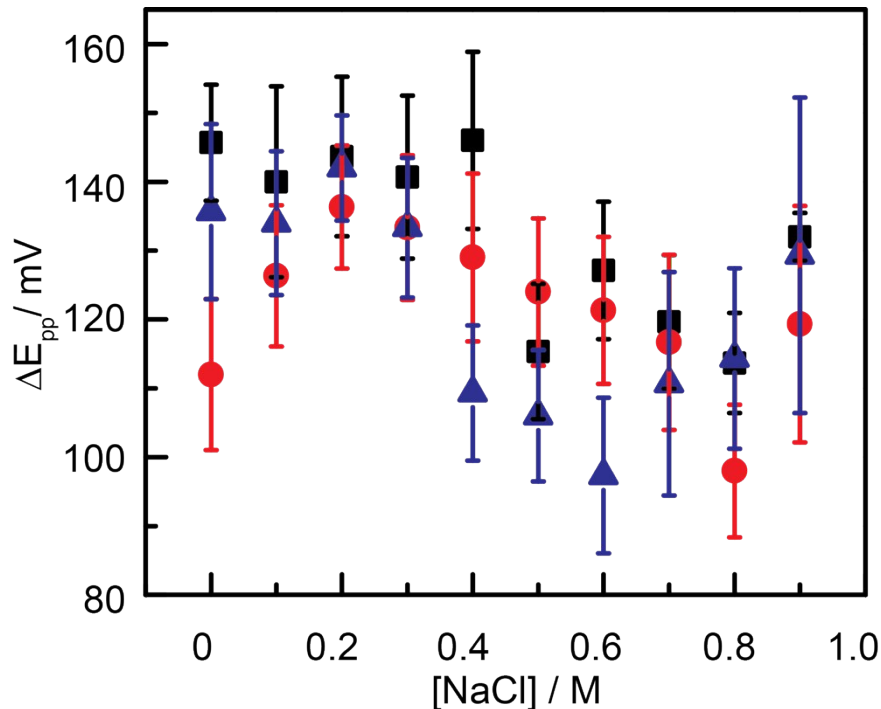


**Figure S6.**  $\Delta E_{pp}$  vs [NaCl] for [Q-SSA][TMA] taken from cyclic voltammograms at 50 mV/sec (red), 100 mV/sec (blue) and 200 mV/sec (black) at pH 4 in 0.1 M acetate buffer.

## DLS data

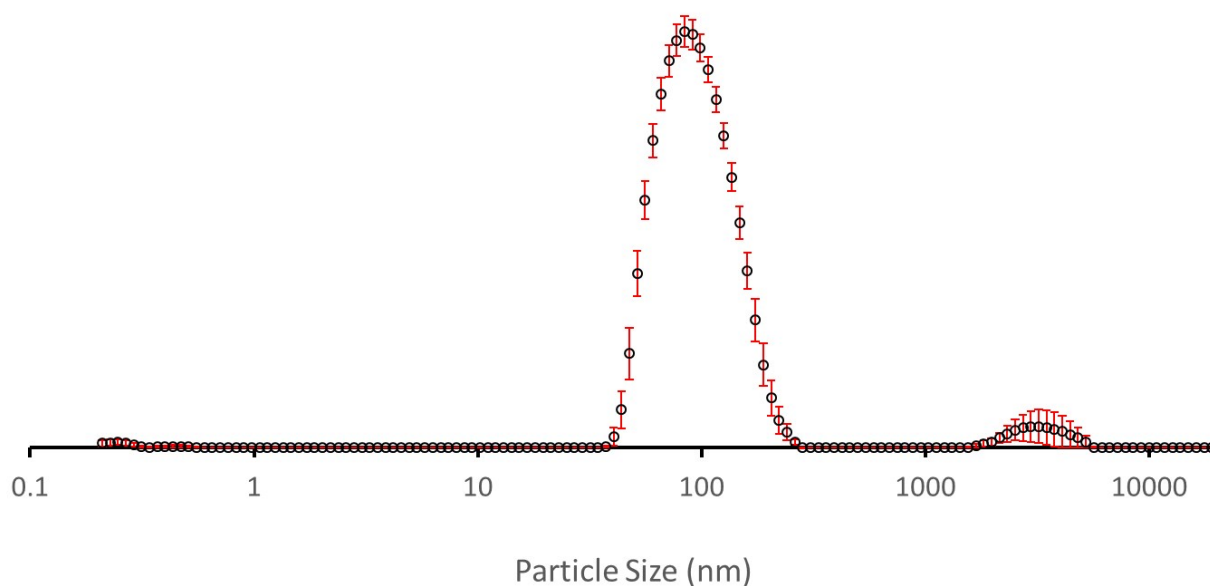


**Figure S7a** – Average intensity particle size distribution, calculated from 9 DLS runs, of aggregates formed by dissolving [Q-SSA][TBA] (1 mg) in an aqueous solution of 0.1 M NaOAc (20 mL), after heating to 40 °C and cooling to 25 °C.

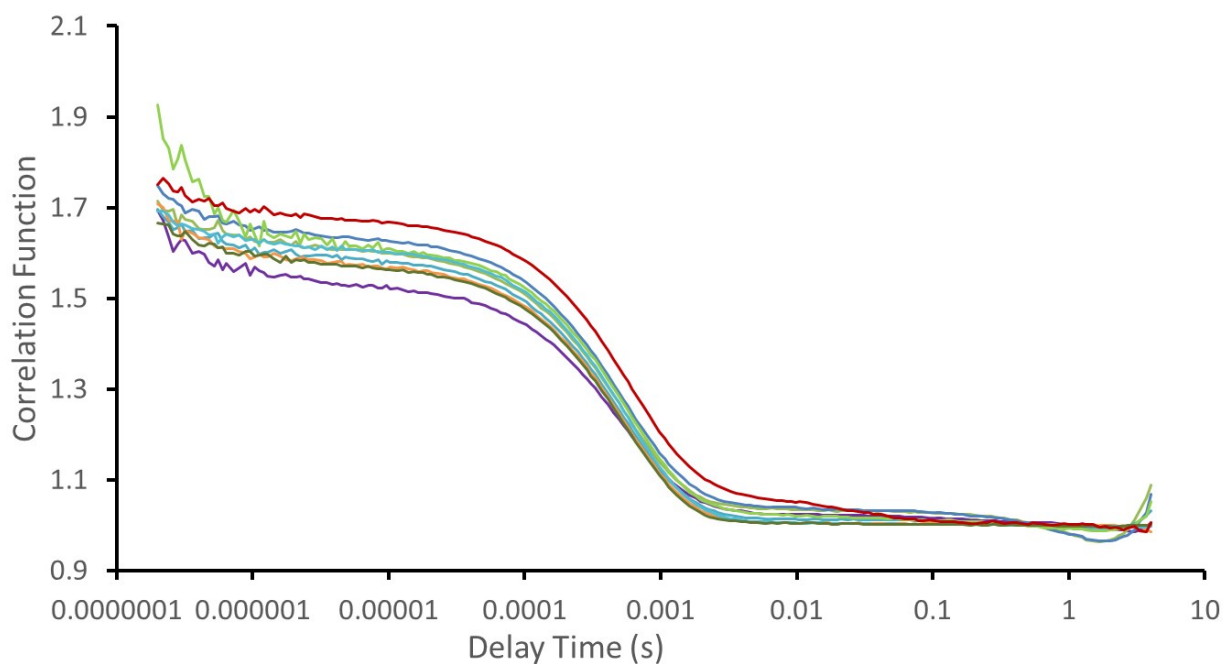


**Figure S7b** – Correlation function data for 9 DLS runs of [Q-SSA][TBA] (1 mg) in an aqueous solution of 0.1 M NaOAc (20 mL), after heating to 40 °C and cooling to 25 °C.

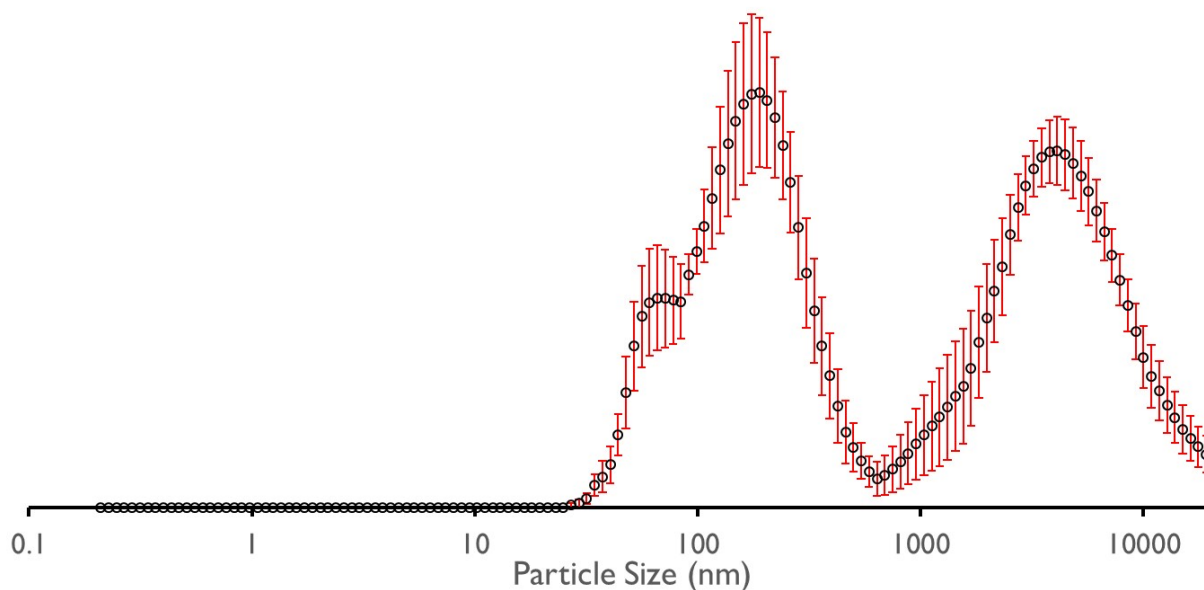


**Figure S8a** – Average intensity particle size distribution, calculated from 9 DLS runs, of aggregates formed by dissolving [Q-SSA][TBA] (1 mg) in an aqueous solution of 0.1 M NaOAc and 0.9 M NaCl (20 mL), after heating to 40 °C and cooling to 25 °C.

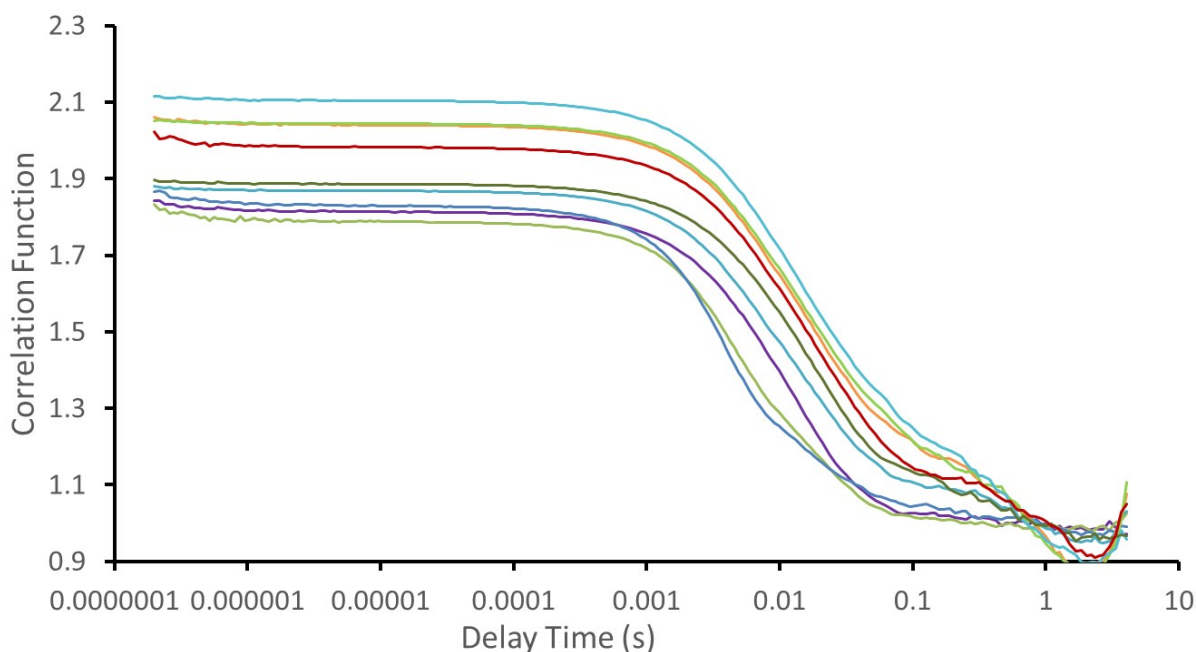


**Figure S8b** Correlation function data for 9 DLS runs of [Q-SSA][TBA] (1 mg) in an aqueous solution of 0.1 M NaOAc and 0.9 M NaCl (20 mL) after heating to 40 °C and cooling to 25 °C.

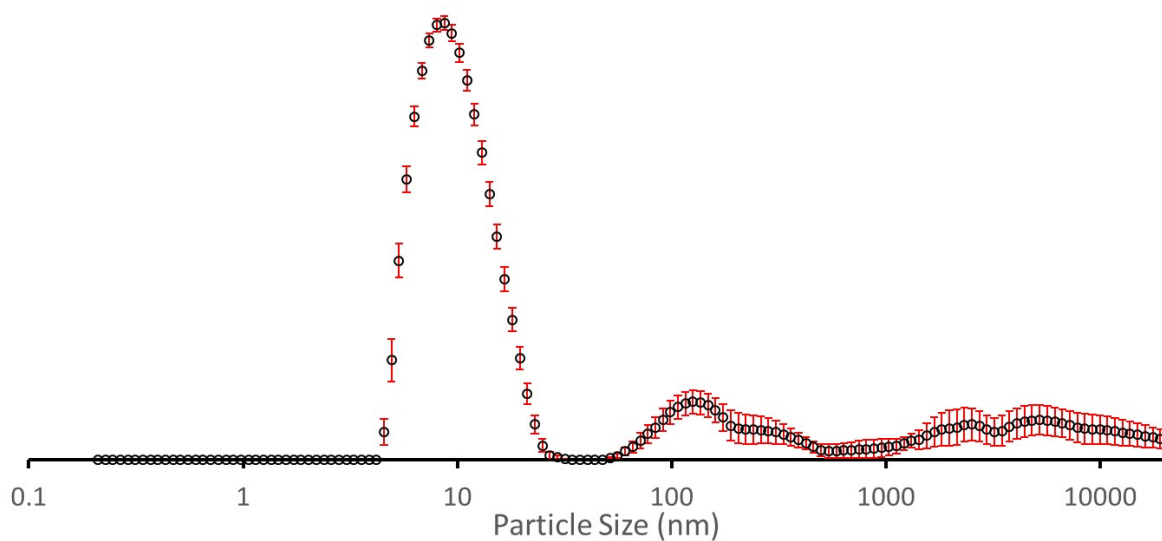


**Figure S9a** – Average intensity particle size distribution, calculated from 9 DLS runs, of aggregates formed by dissolving [Q-SSA][TMA] (1 mg) in an aqueous solution of 0.1 M NaOAc (20 mL), after heating to 40 °C and cooling to 25 °C.

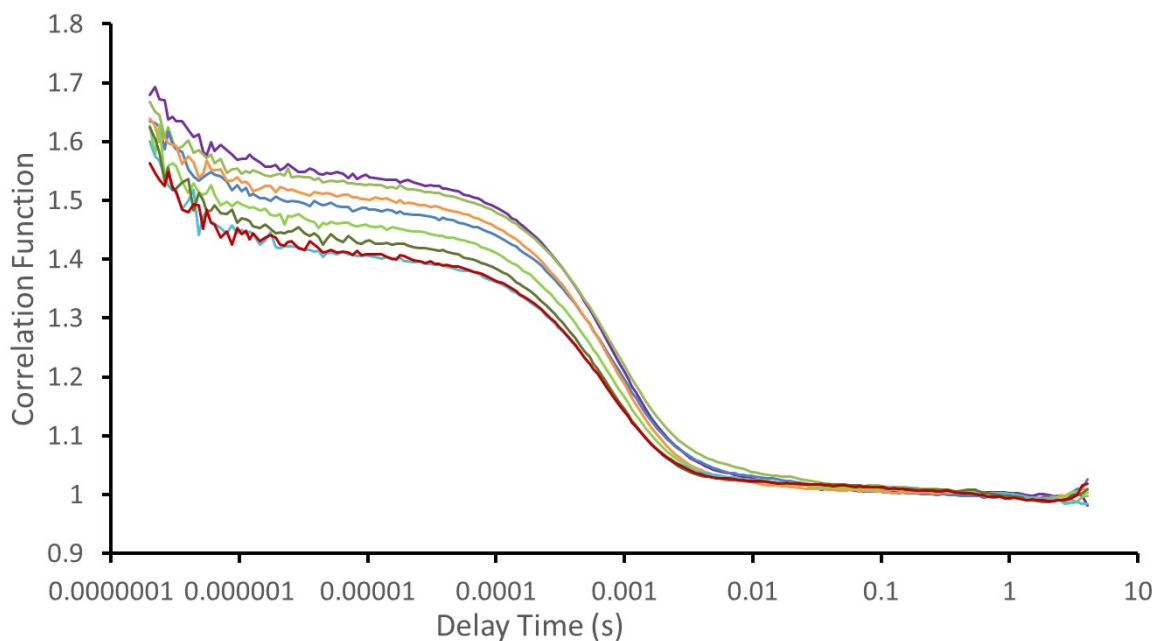


**Figure S9b** – Correlation function data for 9 DLS runs of [Q-SSA][TMA] (1 mg) in a solution of 0.1 M NaOAc (20 mL), after heating to 40 °C and cooling to 25 °C.

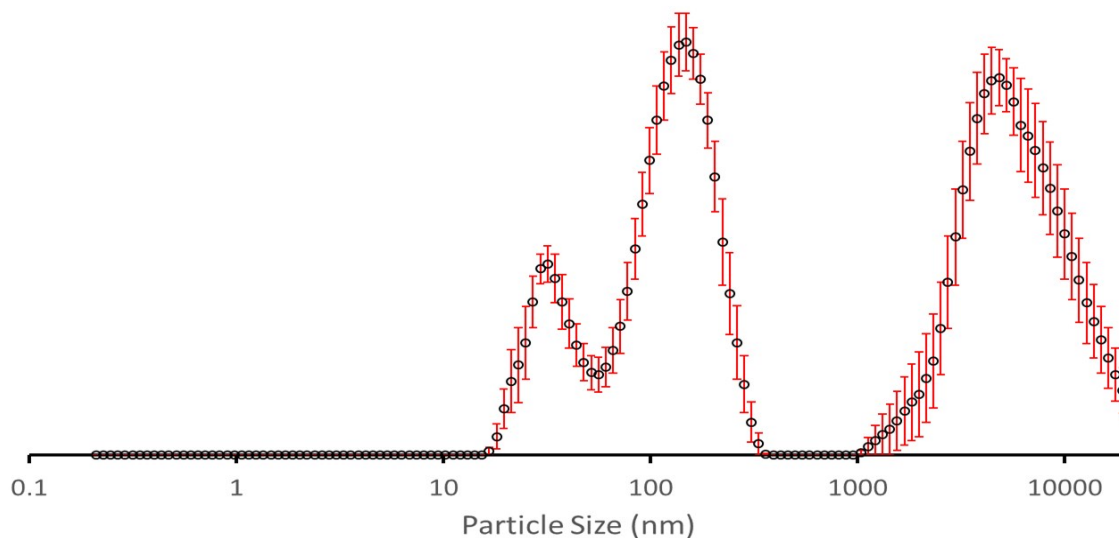


**Figure S10a** – Average intensity particle size distribution, calculated from 9 DLS runs, of aggregates formed by dissolving [Q-SSA][TMA] (1 mg) in an aqueous solution of 0.1 M NaOAc and 0.9 M NaCl (20 mL), after heating to 40 °C and cooling to 25 °C.

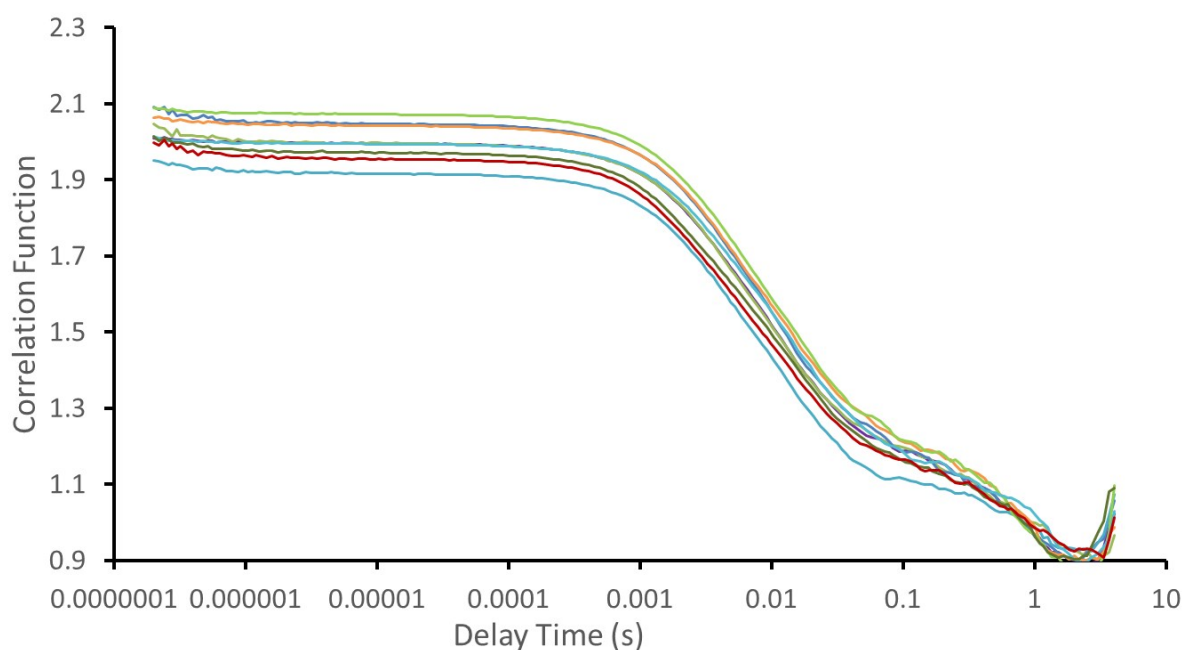


**Figure S10b** – Correlation function data for 9 DLS runs of [Q-SSA][TMA] (1 mg) in an aqueous solution of 0.1 M NaOAc and 0.9 M NaCl (20 mL), after heating to 40 °C and cooling to 25 °C.

### Zeta potential data

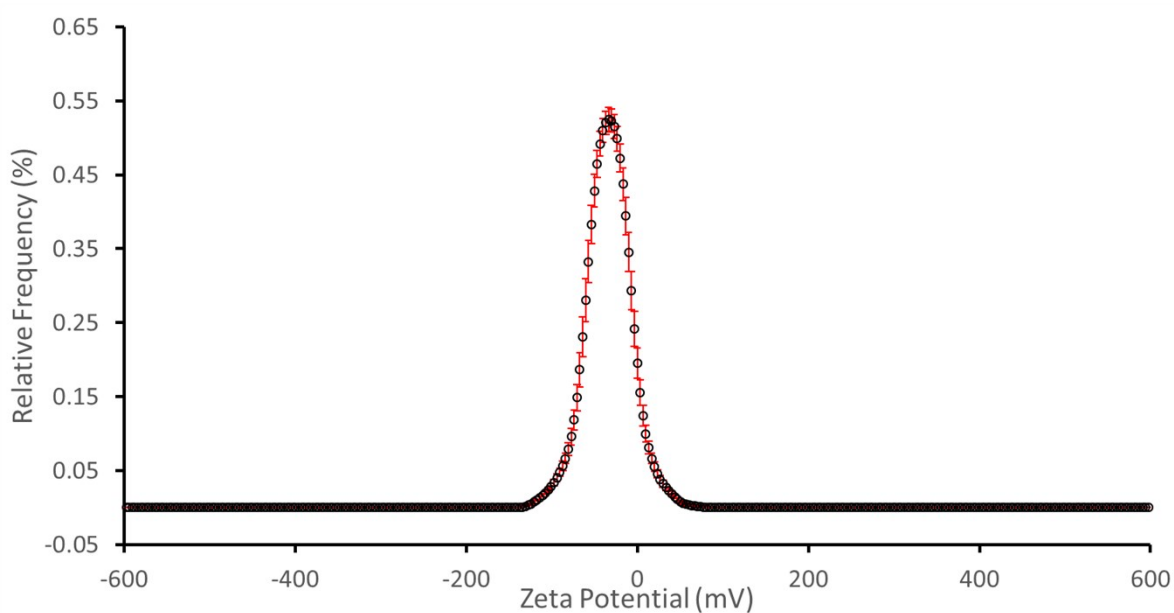


**Figure S11** – The average zeta potential distribution calculated using 10 runs for [Q-SSA][TBA] (1 mg) in an aqueous solution of 0.1 M NaOAc (20 mL) at 25 °C, after heating to 40 °C. Zeta potential = -36.58 mV.

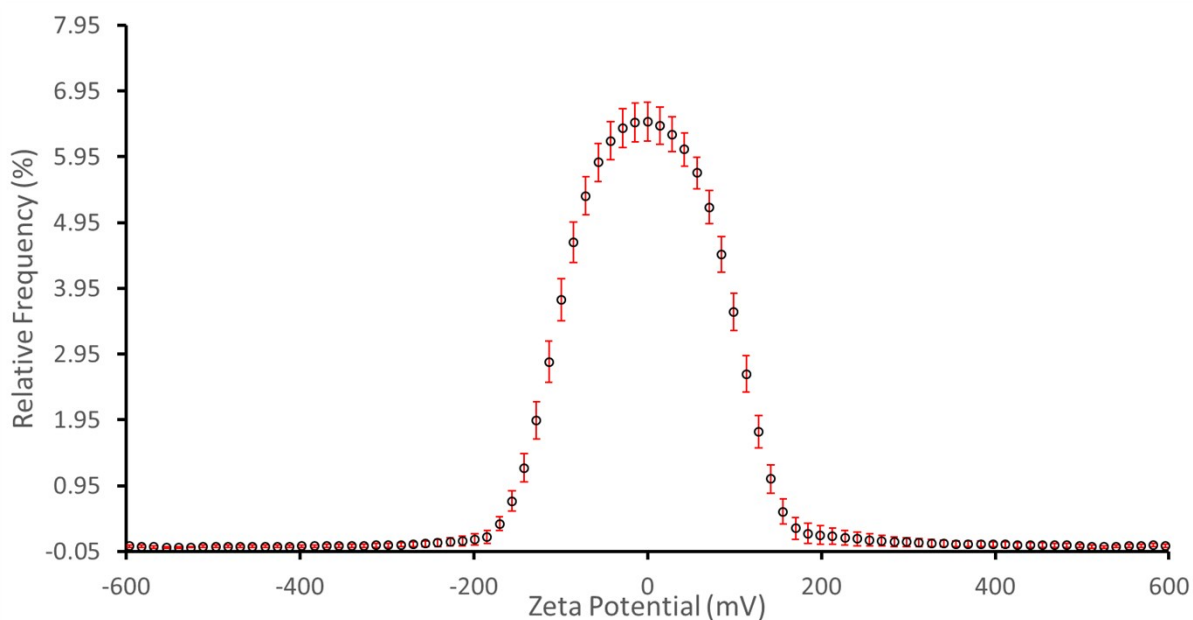


**Figure S12** – The average zeta potential distribution calculated using 10 runs for [Q-SSA][TBA] (1 mg) in an aqueous solution of 0.1 M NaOAc and 0.9 M NaCl (20 mL) at 25 °C, after heating to 40 °C. Zeta potential = -25.88 mV.

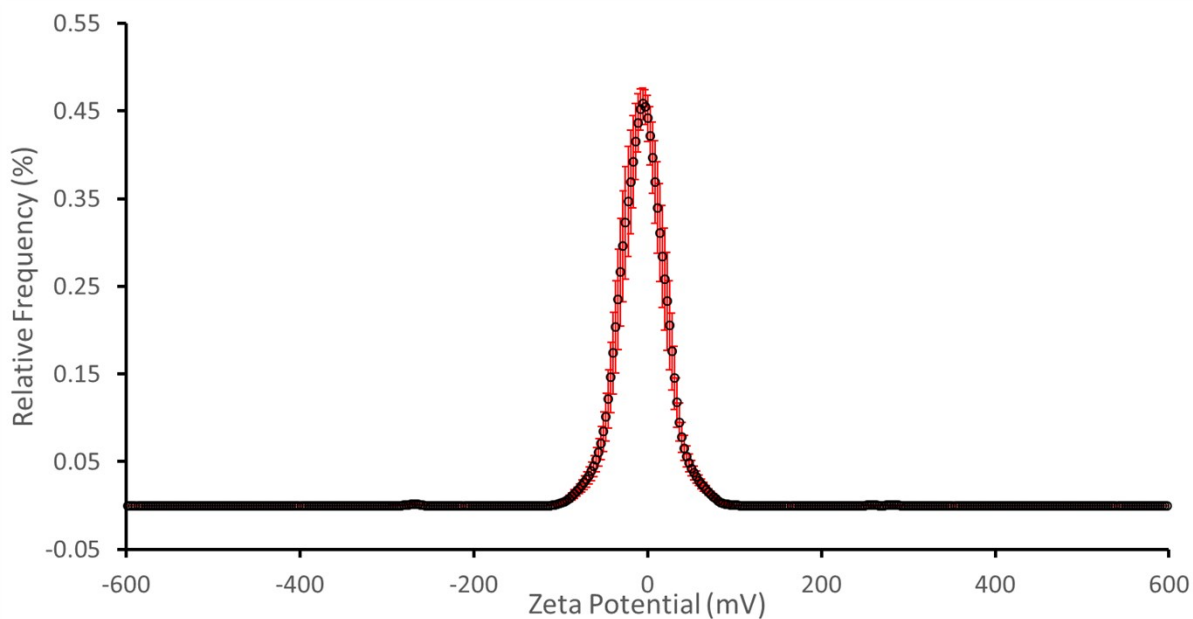


**Figure S13** – The average zeta potential distribution calculated using 10 runs for [Q-SSA][TMA] (1 mg) in an aqueous solution of 0.1 M NaOAc (20 mL) at 25 °C, after heating to 40 °C. Zeta potential =  $-14.97$  mV.

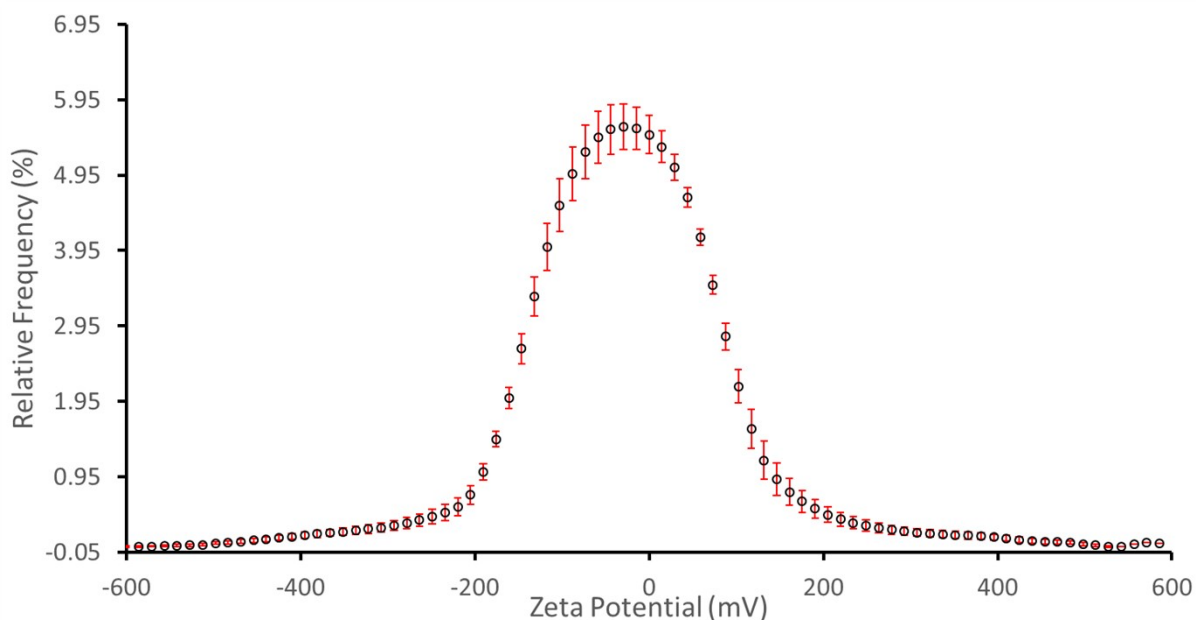


**Figure S14** – The average zeta potential distribution calculated using 10 runs for [Q-SSA][TMA] (1 mg) in an aqueous solution of 0.1 M NaOAc and 1.0 M NaCl (20 mL) at 25 °C, after heating to 40 °C. Zeta potential =  $-32.04$  mV.

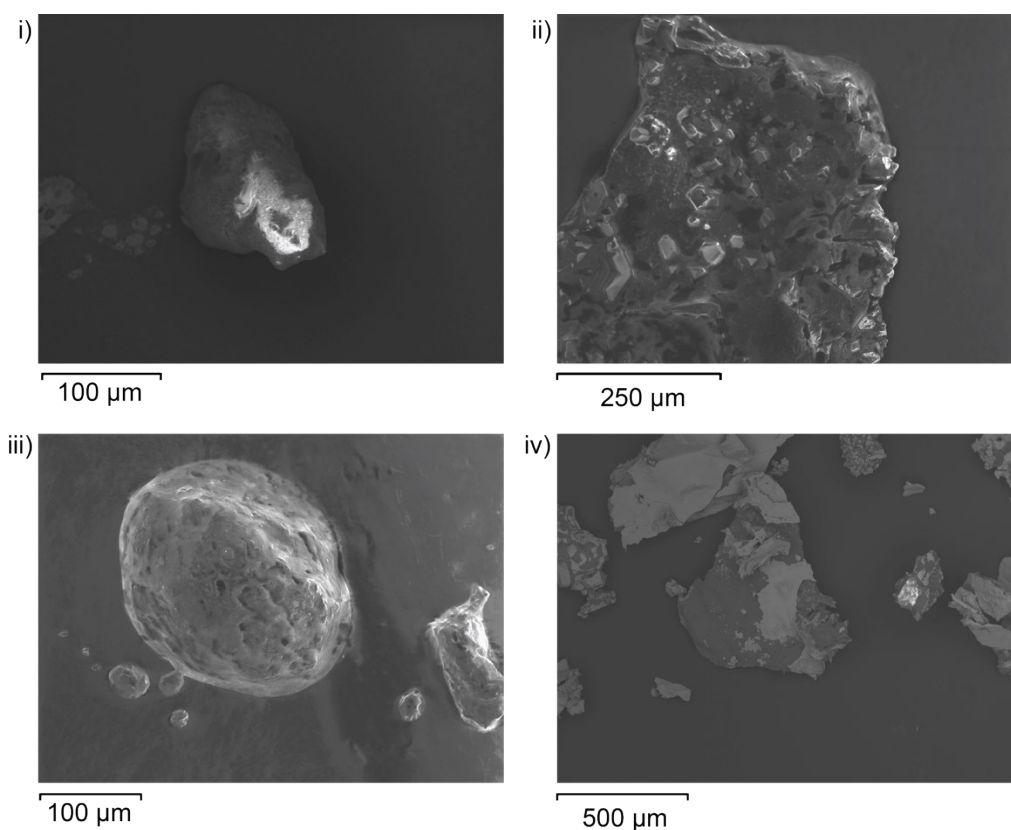


**Figure S15.** SEM images of i) [Q-SSA][TBA] (0.1 M NaOAc), ii) [Q-SSA][TBA] (0.1 M NaOAc, 0.9 M NaCl), iii) [Q-SSA][TMA] (0.1 M NaOAc), iv) [Q-SSA][TMA] (0.1 M NaOAc, 0.9 M NaCl). Shown are largest particles observed which contain appreciable organics as determined by presence of sulfur (only present in the anionic component of the SSA) observed by EDX.

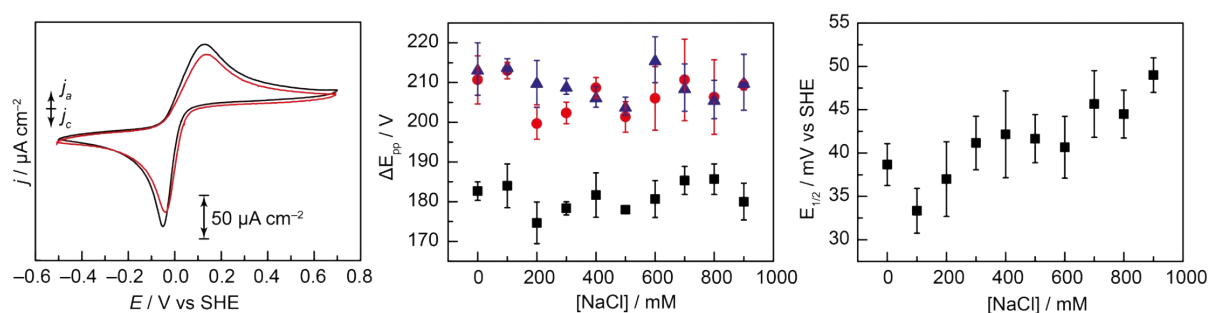


**Figure S16.** Cyclic voltammogram of anthraquinone-2,7-disulfonic acid (AQDS) (0.3 mM) in 0.1 M NaOAc at pH 4 (black) and 0.1 M NaOAc + 0.9 M NaCl (red) (left),  $\Delta E_{pp}$  vs [NaCl] for AQDS, taken from cyclic voltammograms at 50 mV/sec (black), 100 mV/sec (red) and 200 mV/sec (blue) at pH 4 in 0.1 M acetate buffer (centre),  $E_{1/2}$  vs [NaCl] for AQDS taken from cyclic voltammograms at 50 mV/sec, at pH 4 in 0.1 M acetate buffer (right)

## Synthesis

**[Q-SSA][TBA]:** Compound was synthesised in line with our previously published methods. Proton NMR were found to match our previously published values.<sup>1</sup> <sup>1</sup>H NMR (400 MHz, 298 K, DMSO-*d*<sub>6</sub>): 0.93 (t, J = 7.34 Hz, 12H), 1.30 (m, 8H), 1.56 (m, 8H), 3.16 (m, 8H), 3.94 (d, J = 5.88 Hz, 2H), 6.90 (m, NH), 7.76 (dd, J = 2.28, 8.60 Hz, 1H), 7.86 (m, 2H), 8.05 (d, J = 8.52 Hz, 1H), 8.12 (m, 2H), 8.27 (m, 1H), 9.59 (m, NH).

**[Q-SSA][TMA]:** A solution of 2-aminoanthraquinone (0.67 g, 3.01 mM) and triphosgene (0.45 g, 1.50 mM) in ethyl acetate (30 mL) was heated at reflux under nitrogen for 4 hours. TMA aminomethane sulfonate (1.06 g, 3.01 mM) in ethyl acetate (10 mL) was then added to the reaction mixture, which was then heated at reflux overnight. The crude product was taken to dryness and water (20 mL) was added and the resultant mixture centrifuged, the supernatant was washed with chloroform (20 mL) and the aqueous layer was taken to dryness. Pure product was precipitated out with methanol, yielding a bright yellow solid. Yield: 8.7% (0.114 g, 0.26 mmol); MP > 200 °C; <sup>1</sup>H NMR (400 MHz, 298 K, DMSO-*d*<sub>6</sub>): 3.09 (s, 12H), 3.93 (d, J = 5.96 Hz, 8H), 6.89 (br s, NH), 7.75 (dd, J = 2.40, 8.72 Hz, 1H), 7.86 (m, 2H), 8.05 (d, J = 8.52 Hz, 1H), 8.12 (m, 2H), 8.27 (br s, 1H), 9.59 (br s, NH); <sup>13</sup>C {<sup>1</sup>H} NMR (100 MHz, 298 K, DMSO-*d*<sub>6</sub>): δ: 54.4 (CH<sub>3</sub>), 56.0 (CH<sub>2</sub>), 113.8 (ArCH), 122.3 (ArCH), 125.7 (ArC), 126.2 (ArCH), 126.4 (ArCH), 127.9 (ArCH), 132.84 (ArCH), 132.9 (ArC), 133.7 (ArC), 133.7 (ArCH), 134.2 (ArCH), 146.5 (ArC), 154.9 (C=O), 180.9 (C=O), 182.3 (C=O); IR (film): ν = 3356, 3030 (NH stretch), 1705, 1666 (C=O stretch), 1340, 1176 (S=O stretch); HRMS for the sulfonate-urea ion (C<sub>15</sub>H<sub>14</sub>N<sub>2</sub>O<sub>6</sub>) (ESI<sup>-</sup>): m/z: act: 358.2461 [M]<sup>-</sup> cal: 359.0343 [M]<sup>-</sup>.

## Compound characterisation

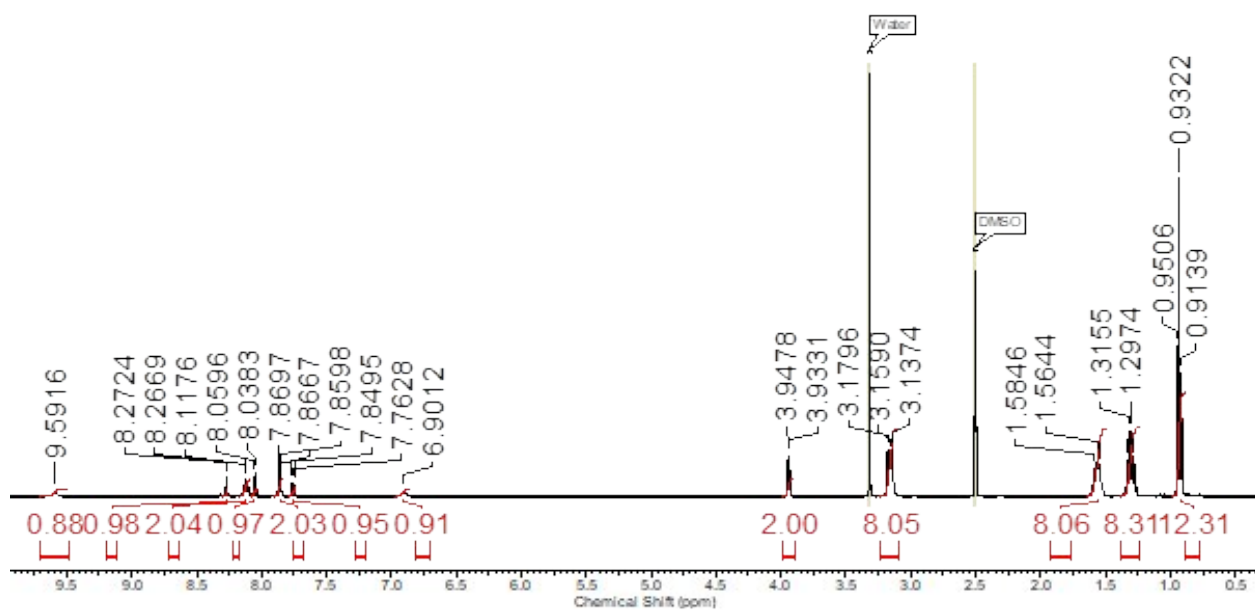


**Figure S17a** <sup>1</sup>H NMR of [Q-SSA][TBA] at 25 °C in DMSO - *d*<sub>6</sub>.

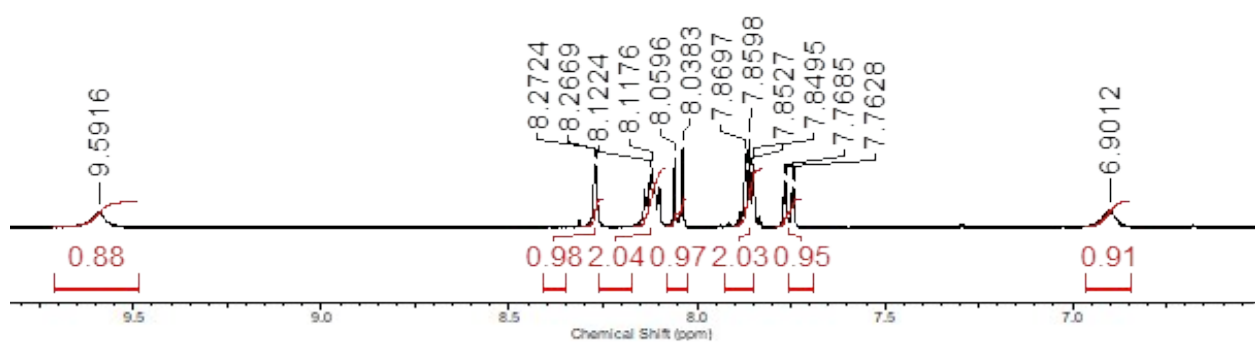


**Figure S17b** – Enlarged <sup>1</sup>H NMR of [Q-SSA][TBA] at 25 °C in DMSO - *d*<sub>6</sub>.

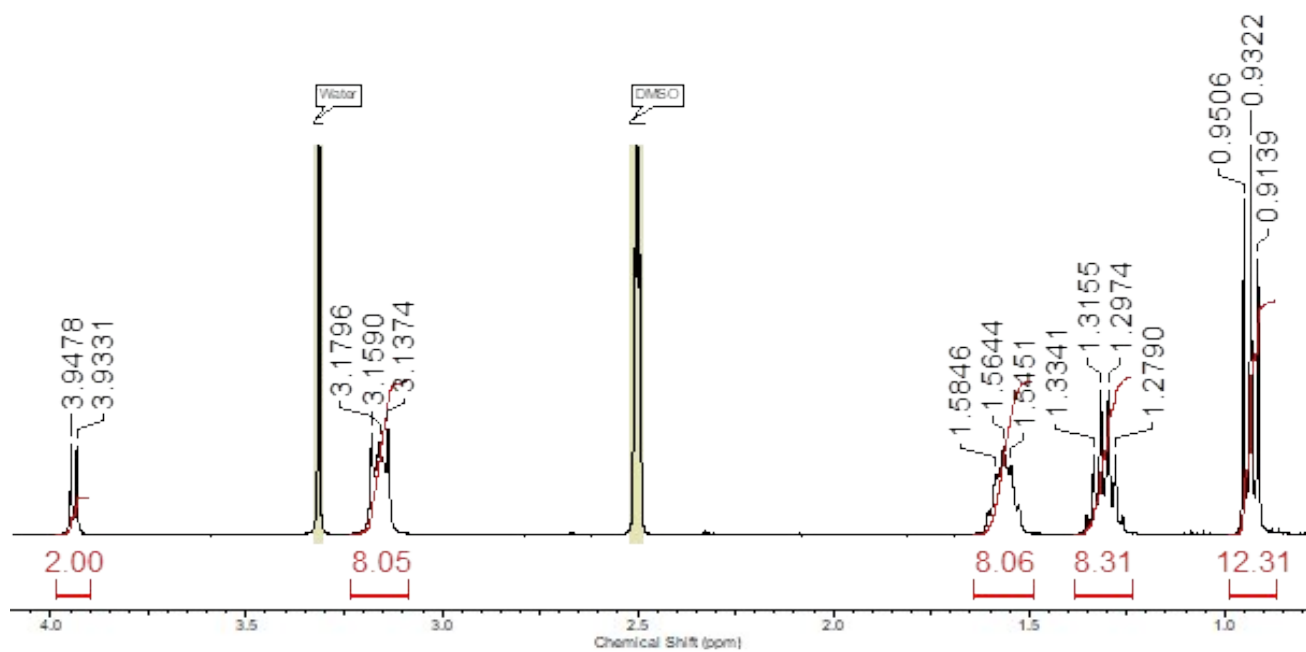


**Figure S17c** Enlarged  $^1\text{H}$  NMR of  $[\text{Q-SSA}][\text{TBA}]$  at  $25\text{ }^\circ\text{C}$  in  $\text{DMSO} - d_6$ .

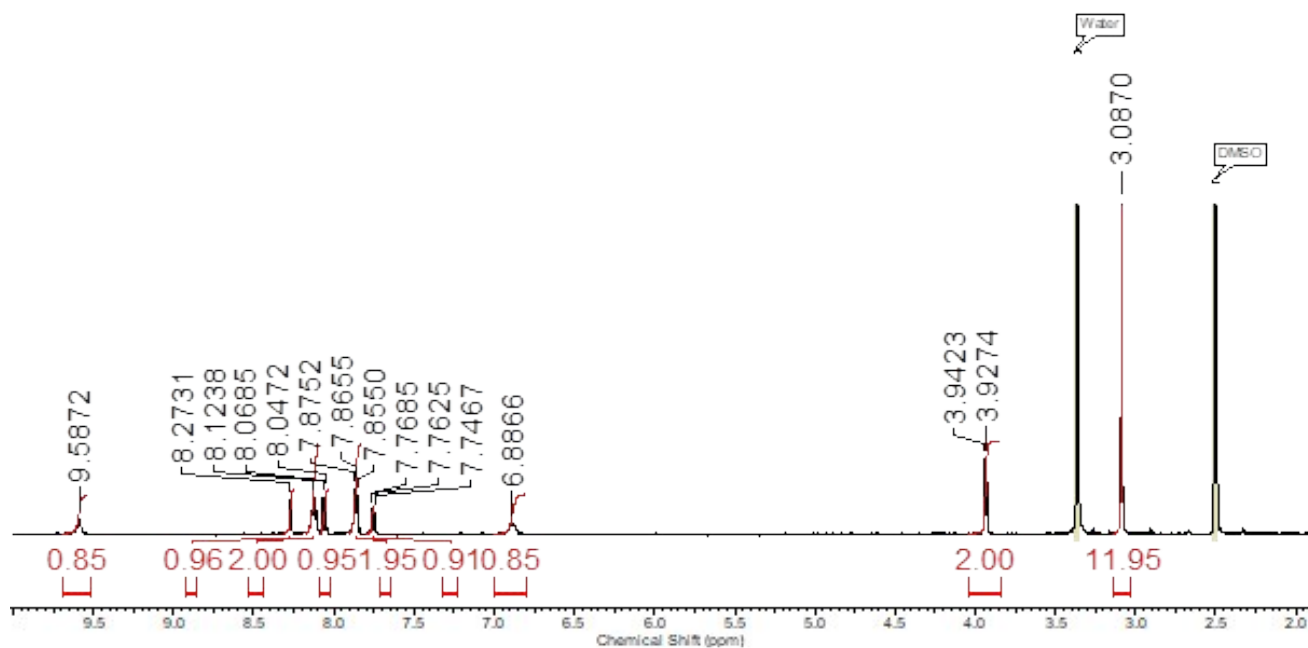


**Figure S18a**  $^1\text{H}$  NMR of [Q-SSA][TMA] at 25 °C in  $\text{DMSO}-d_6$ .

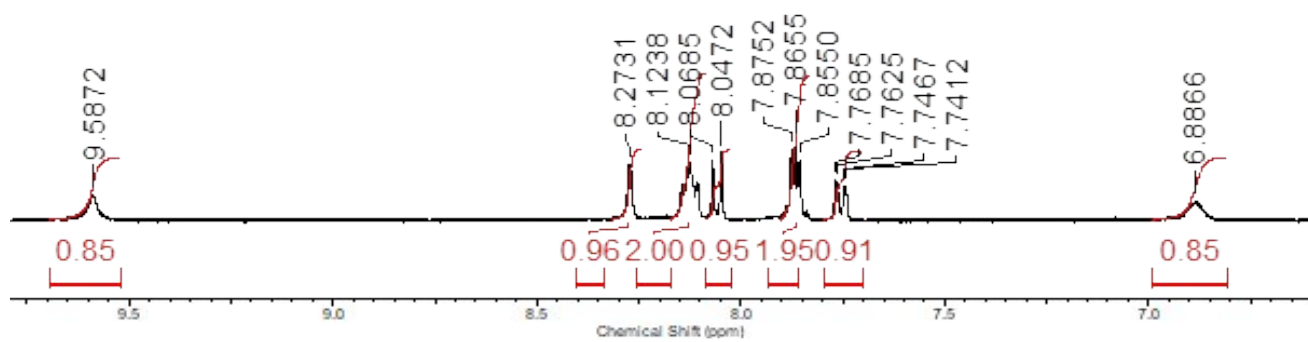


**Figure S18b** – Enlarged  $^1\text{H}$  NMR of [Q-SSA][TMA] at 25 °C in  $\text{DMSO}-d_6$ .

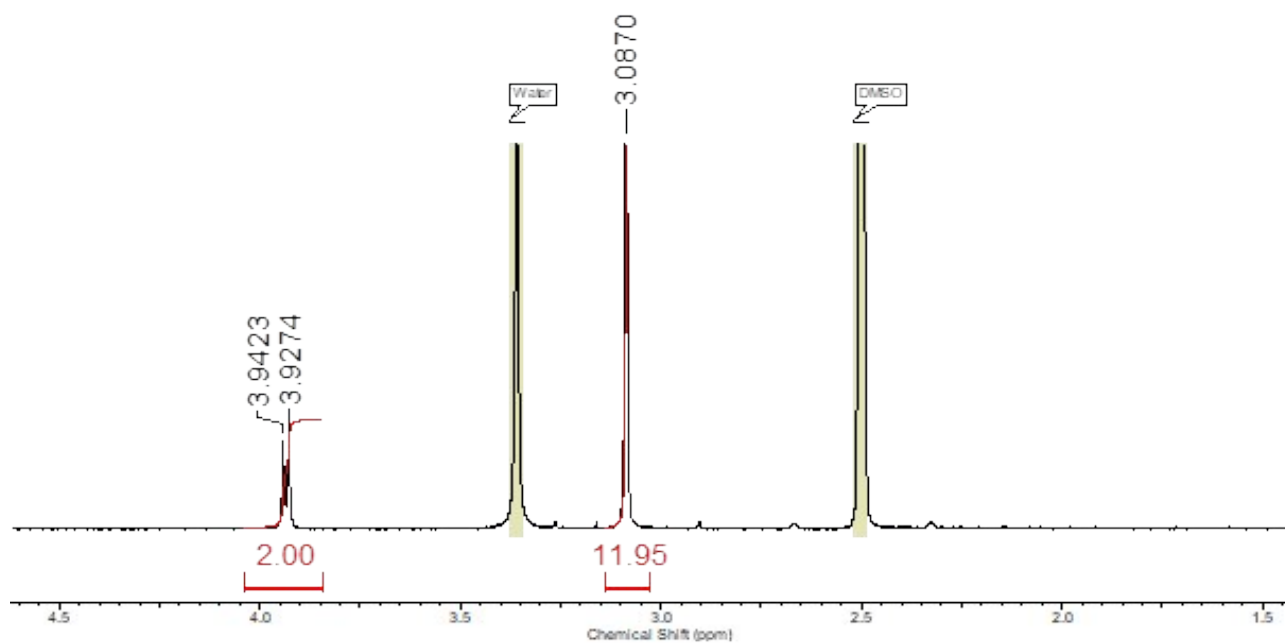


**Figure S18c** – Enlarged  $^1\text{H}$  NMR of [Q-SSA][TMA] at 25 °C in  $\text{DMSO}-d_6$ .

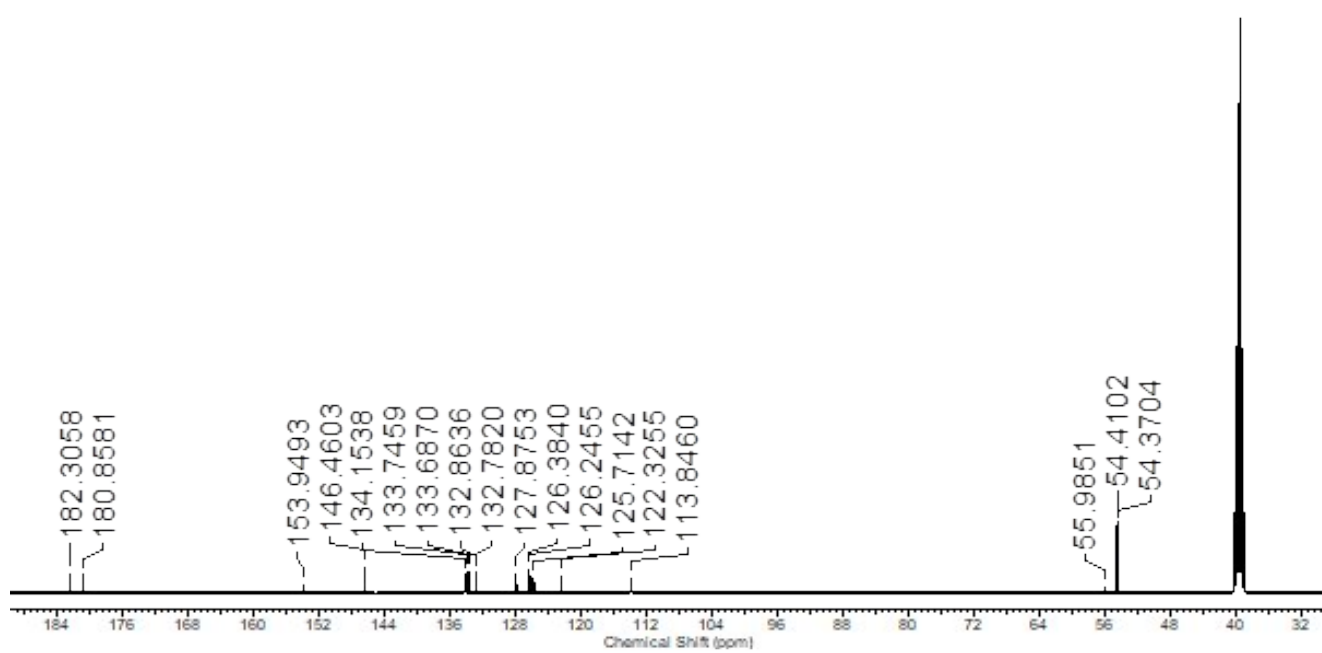


**Figure S19a** –  $^{13}\text{C}\{^1\text{H}\}$  NMR of [Q-SSA][TMA] at 25 °C in  $\text{DMSO}-d_6$ .

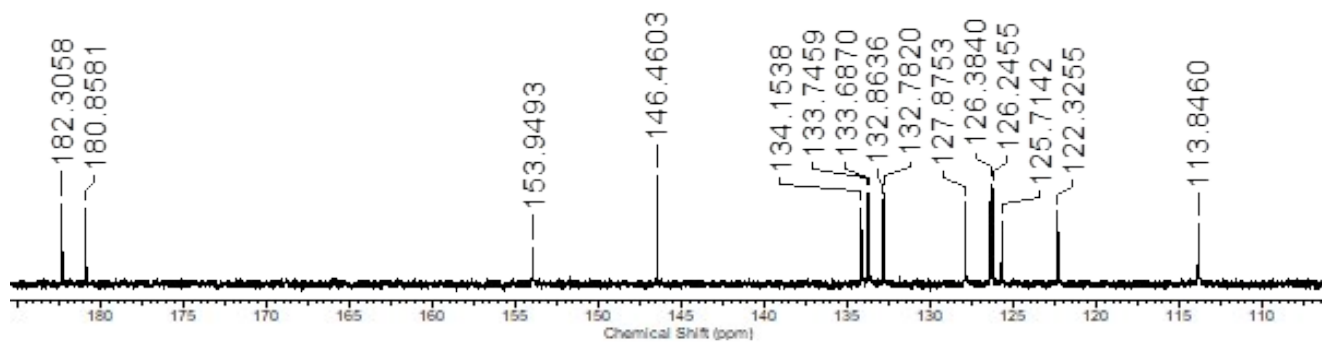


**Figure S19b** Enlarged  $^{13}\text{C}\{^1\text{H}\}$  NMR of [Q-SSA][TMA] at 25 °C in DMSO -  $d_6$ .

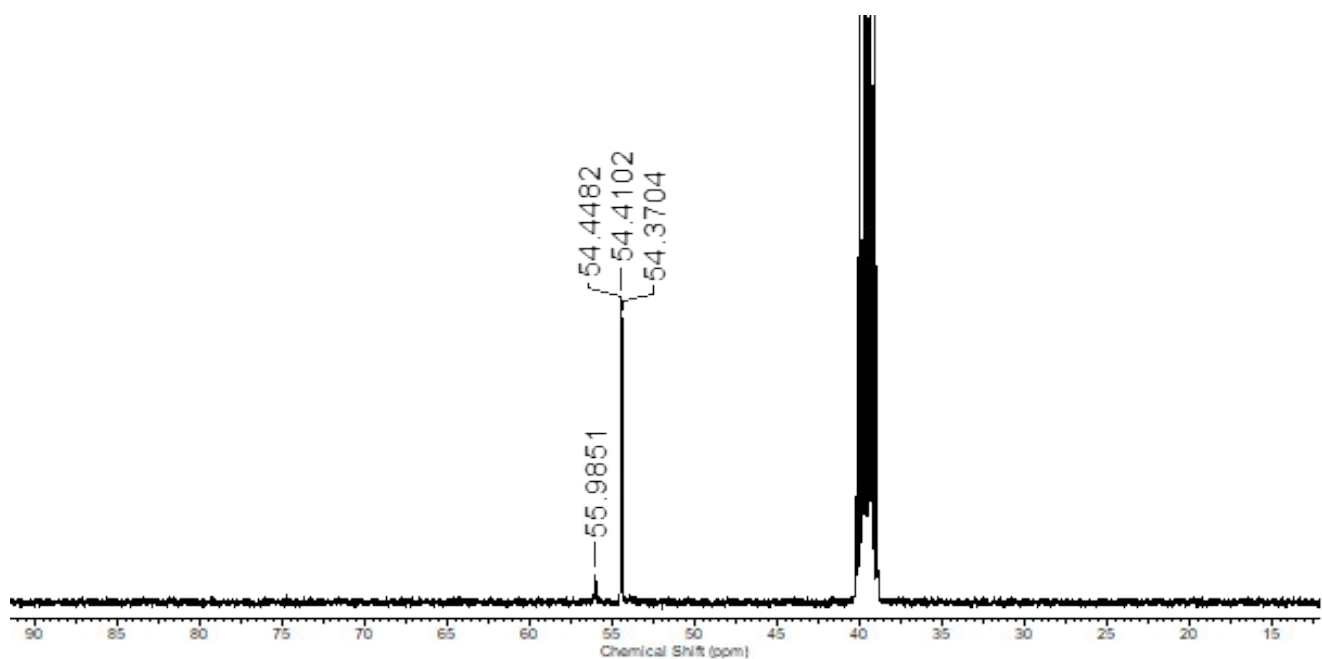


**Figure S19c** – Enlarged  $^{13}\text{C}\{^1\text{H}\}$  NMR of [Q-SSA][TMA] at 25 °C in DMSO -  $d_6$ .

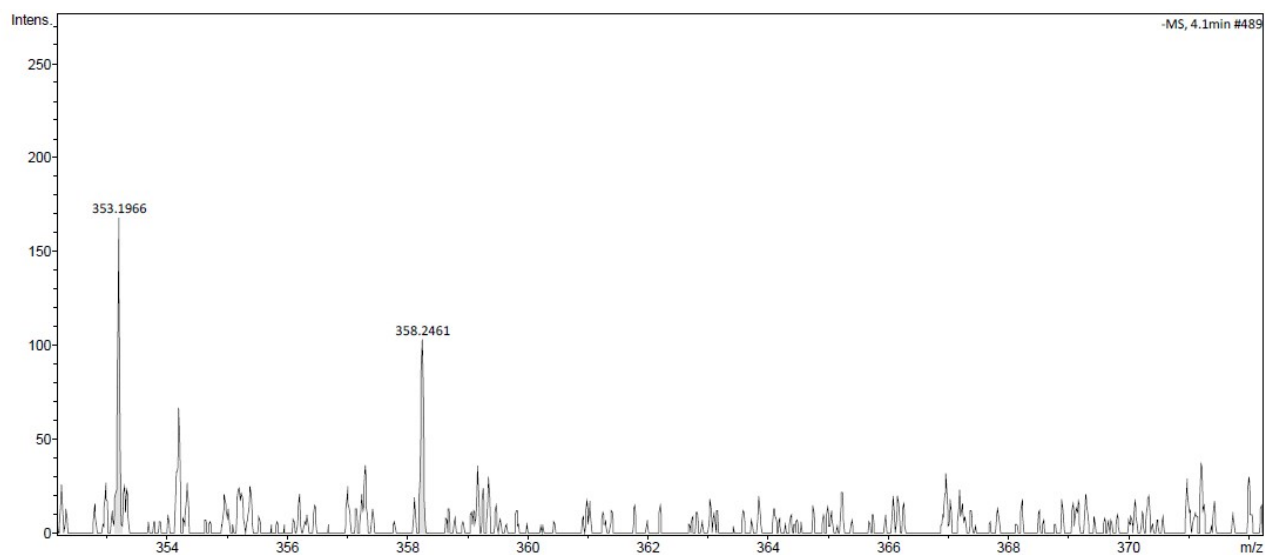


**Figure S20**High-resolution ESI -ve mass spectrometry data obtained for [Q-SSA][TMA].

## References

- 1 S. N. Tyuleva, N. Allen, L. J. White, A. P  p  s, H. J. Shepherd, P. J. Saines, R. J. Ellaby, D. P. Mulvihill and J. R. Hiscock, *Chem. Commun.*, 2019, **55**, 95–98.